NASA TECHNICAL MEMORANDUM

NASA TM X-1706

NASA TM X-1706

PRELIMINARY INVESTIGATION OF DISTORTION DYNAMICS IN A MACH 3 MIXED-COMPRESSION INLET

by Robert E. Coltrin and Glenn A. Mitchell

Lewis Research Center

Cleveland, Ohio

NATIONAL AERONAUTICS AND SPACE ADMINISTRATION • WASHINGTON, D. C. • DECEMBER 1968

NASA TM X-1706

PRELIMINARY INVESTIGATION OF DISTORTION DYNAMICS IN A MACH 3 MIXED-COMPRESSION INLET

By Robert E. Coltrin and Glenn A Mitchell

Lewis Research Center
Cleveland, Ohio

NATIONAL AERONAUTICS AND SPACE ADMINISTRATION

For sale by the Clearinghouse for Federal Scientific and Technical Information
Springfield, Virginia 22151 – CFSTI price $3.00

ABSTRACT

The inlet was operated at critical and supercritical conditions while at 0^{o} angle of attack in the 10- by 10-foot supersonic wind tunnel. The cowl lip diameter was 45.98 cm. Total-pressure sensors with a flat response to 200 Hz were distributed at several diffuser exit locations. The amplitude probability density functions for the total pressures were nearly Gaussian. Frequency analysis showed that the amplitude of the power spectral densities for these pressures dropped by half from 0 to 100 Hz, but was nearly constant at higher frequencies. No periodic components were observed.

PRELIMINARY INVESTIGATION OF DISTORTION DYNAMICS IN A MACH 3 MIXED-COMPRESSION INLET

by Robert E. Coltrin and Glenn A. Mitchell

Lewis Research Center

SUMMARY

Dynamic total-pressure measurements were obtained at several diffuser exit locations of a Mach 3 mixed-compression inlet. The inlet was operated at critical and various supercritical shock positions while at 0° angle of attack in the 10- by 10-foot supersonic wind tunnel. The cowl lip diameter was 45.98 centimeters. Total pressure sensors with a flat response to 200 hertz were located at the simulated compressor face. Total-pressure amplitude probability densities indicated the data were nearly Gaussian. Frequency analysis showed that the amplitude of the power spectral densities for these pressures dropped by half from 0 to 100 hertz, but was nearly constant at higher frequencies. No periodic components were observed.

INTRODUCTION

It has long been recognized that the flow from a supersonic diffuser may have a serious total-pressure distortion at the compressor face which can influence the engine stall margin. More recently it has become apparent that total-pressure fluctuations are superimposed upon the steady distortion and may further alter the compressor stall margin. This dynamic distortion apparently originates from the unsteady interaction of the diffuser terminal shock with the inlet boundary layer which produces localized three-dimensional transients in flow velocity and direction at the diffuser exit. The effects of this dynamic distortion on a compressor stall margin are presented in reference 1. These distortion dynamics were created artificially in a supersonic-inlet simulator which utilized a choke point in an engine-connected pipe test stand. Shock waves downstream of this choke point interacted dynamically with the duct boundary layer. Only limited data are presently available that define the distortion dynamics which actually exist within an inlet at supersonic speeds. Therefore, the present study was undertaken to briefly define the

qualitative aspects of distortion dynamics existing in a typical supersonic inlet. The investigation was conducted in the Lewis 10- by 10-foot supersonic wind tunnel at Mach 3 with an axisymmetric, mixed-compression inlet. The Reynolds number based on cowl lip diameter was 3.75 million. Although it is recognized that flow directionality fluctuations may be important, the instrumentation was limited to diffuser exit total-pressure transducers.

SYMBOLS

A	area, cm^2
F(y)	probability density function

$$\lim_{T\to\infty} \lim_{\Delta y\to 0} \frac{1}{T(\Delta y)} \sum_{l=1}^{\infty} t_l(y,\ y + \Delta y)$$

f	frequency, Hz
Δf	filter bandwidth used in spectral analysis, Hz
L	length of subsonic diffuser, cm
M	Mach number
m	mass flow, kg/sec
P	time-averaged total pressure, N/m^2 abs
$PSD_i(f)$	power spectral density,

$$\lim_{T\to\infty} \lim_{\Delta f\to 0} \frac{1}{T(\Delta f)} \int_0^T \left(\Delta P_i\right)^2_{\Delta f}\, dt$$

in the frequency band from f to f + Δf, $\left(N/m^2\right)^2/Hz$

ΔP	fluctuating component of total pressure, N/m^2
$(\Delta P_i)_{\Delta f}$	amplitude of total-pressure fluctuation at location i within a frequency band from f to f + Δf, N/m^2
r	radius
T	time length of data reduced for probability density and spectral analysis, sec
t	time, sec

$t_{\ell}(y,\ y + \Delta y)$	time spent by pressure during its ℓ^{th} entry into a band between amplitude gates, at pressures of y and $y + \Delta y$, sec
x	linear distance, cm
y	level of pressure amplitude gate for probability density function, N/m^2
σ	standard deviation

$$\left(\frac{1}{T}\int_0^T \Delta P^2\, dt\right)^{1/2}$$

Subscripts:

a, b, c, d	sensor locations on diffuser exit rakes
Δf	filter bandwidth used in spectral analysis, Hz
i	arbitrary dummy variable
ℓ	cowl lip station
max	maximum
min	minimum
rms	root-mean-square value
x	conditions at x-distance
0	free-stream station
2	diffuser exit station (compressor face)

Superscript:

(-)	area-weighted average

APPARATUS AND PROCEDURE

Model

The Mach 3 mixed-compression inlet is shown in figure 1. A schematic diagram of its aerodynamic design is presented in figure 2. Further details of its design and performance are reported in references 2 and 3. For supersonic compression, it utilized an isentropic spike with an initial cone half angle of 13.65°. The spike compression waves were focused at the cowl lip. Internal contraction was generated by the compressive turning of the inner cowl surface which created two oblique shocks focused at the

boundary-layer bleed slot on the centerbody. At the design conditions, the average throat Mach number ahead of the terminal shock was 1.45. The initial part of the subsonic diffuser was provided with two hydraulic diameters of essentially constant area and was followed by an equivalent 12° conical area expansion to the simulated compressor face approximately 1.5 inlet diameters from the cowl lip. The resulting internal area variation of the diffuser is shown in figure 3.

Instrumentation

In addition to the normal steady-state instrumentation of the inlet described in reference 2, four dynamic sensors were placed in two of the total-pressure rakes located at the simulated compressor face. Their relative positions are shown in figure 4(a). It should be noted that the two rakes were on opposite sides of the centerbody support struts which essentially divided the subsonic diffuser in half over a substantial portion of its length.

The construction of the dynamic pressure sensor is illustrated in figure 4(b). Since the piezoelectric-type transducers were too large to be placed directly in the total-pressure rakes, all transducers were mounted to 15.2-centimeter-long tubes so that the transducer cases could be attached to the exterior of the diffuser wall. The pneumatic system of the pressure sensor was designed to obtain a damped second-order system with a relatively flat response to 200 hertz. This was accomplished for the tube length of 15.2 centimeters by properly matching the tube diameter of 0.038 centimeter to the volume of the cavity at the transducer face. This cavity volume was controlled by compression of the paper gaskets indicated in figure 4(b) which total 0.114 centimeter thick before compression. The sensitivity of the sensor frequency response to changes in cavity volume is shown in figure 5(a) where the normalized amplitude ratio was evaluated as the measured amplitude at the test frequency ratioed to the measured amplitude at the sensor inlet. The response is given for a sensor with gasket compression to 0.069 and 0.025 centimeter. Three typical sensors with gaskets compressed to the design value of 0.069 centimeter were calibrated and their frequency response is shown in figure 5(b). The four sensors placed in the model for the test were identical to these but could not be individually calibrated because they were assembled in the model and were inaccessible.

During the course of wind tunnel testing, it was determined that the pressure oscillations which occur during inlet unstart and buzz were too severe for the sensor construction of figure 4(b). The paper gaskets began to leak and changed the designed probe response. The results presented subsequently in this report were obtained prior to an inlet unstart and appeared to be leak-free for these operating conditions. Subsequent examination of the probes revealed that the only effect of the leaks was to uniformly reduce

the measured amplitudes throughout the 0- to 200-hertz range. Thus, the qualitative aspects of the data presented herein are not in question. However, for subsequent testing, an improved sensor design is required.

Data Analysis

Dynamic data were recorded directly on magnetic tape. It was recognized that the frequency response of the pneumatic pressure-sensing systems had unwanted resonances at high frequencies (greater than 200 Hz) which is typical of a transmission line or distributed-parameter-type system. Therefore, the data were transferred to a second magnetic tape through a fourth-order filter made up of two second-order filters each with a natural frequency of 200 hertz and a damping ratio of 0.7.

Amplitude probability densities of the pressure fluctuations were obtained by analyzing 20 seconds of filtered tape on analog equipment. An amplitude segment (or amplitude gate width) of one-fourth the rms value was selected which partitioned the peak-to-peak amplitude into 24 segments. The rms values were obtained by an rms voltmeter reading from the filtered tape. The value of the standard error calculated for amplitude probability densities computed in this manner is less than 2 percent, where the probability density is near 0.4 (mean value of $\Delta P/P_{rms}$) and about 9 percent where the probability density is near 0.005 (peak values of $\Delta P/P_{rms}$). That is to say, with 68 percent confidence, the true value of the amplitude probability density is within ±2 percent or ±9 percent of the measured value at probability density values near 0.4 and 0.005, respectively. The mean value of all the amplitude probability density plots is zero because the piezoelectric sensors measure only the fluctuating component of the pressure.

Power spectral density functions were obtained for the pressure fluctuations by analyzing 30 seconds of unfiltered tape on analog equipment using 2-hertz bandwidths. The data were not analyzed beyond the 200-hertz probe limit. Typical errors were calculated to be 15 percent at an 80 percent level of confidence and 20 percent at a 90 percent level of confidence. An rms value can be computed for each spectrum from the square root of the area under the power spectral density curve. It was determined that these values were close (within the computed error) to the values obtained from an rms reading of the filtered tape, indicating that the measured power spectra were reasonably accurate.

In order to reduce the data by the methods described above, the data must be stationary. A simple nonparametric test for stationarity involving an investigation of the scatter of the mean square pressure measurements was performed on the data. The results showed that within the limits of this test, the data were indeed stationary.

RESULTS AND DISCUSSION

The steady-state performance of the inlet at 0^{o} angle of attack is shown in figure 6. Data for four operating conditions are shown, and of these the critical point and the two most supercritical points were selected for detailed analysis of distortion dynamics. Critical is defined as the operating point with the terminal shock at the inlet throat. The supercritical values quoted are defined as the drop in total-pressure recovery from the critical value computed as a percentage of the critical value. Steady-state distortion maps corresponding to these conditions are shown in figure 7. For the remaining figures of this report, two dynamic sensors were selected for analysis at each of the three operating conditions. The locations of these sensors within the distorted flow are also indicated in figure 7. At critical conditions they were widely separated on different rakes (a and b), at the 9 percent supercritical condition they were closely spaced on the same rake (b and c), and at 13 percent supercritical they were widely spaced on the same rake (b and d).

Evidence of the randomness of the measured pressure amplitudes at frequencies below 200 hertz is shown in figure 8 where the experimental amplitude probability densities for the various operating conditions are compared with the Gaussian density. It is apparent that the experimental results were essentially Gaussian and, thus, there was no evidence of periodic content in the measured frequency range. Therefore, since these data appear to be Gaussian, the peak-to-peak pressure fluctuations can be assumed to be six times the rms values (6 σ for Gaussian data) for frequencies below 200 hertz in this inlet. In order to generalize this result to other inlets, it should first be determined that the amplitude probability densities of the pressures in the selected inlet are Gaussian.

Power spectral densities of the pressure fluctuations, divided by the local total pressure squared, are shown in figure 9 as a function of frequency. All the spectra show an initial drop in power as frequency increased, but they then tended to a constant level before 200 hertz. The initial drop is usually complete by about 100 hertz and is a maximum overall reduction of about half. This is in sharp contrast to the larger-scale inlet simulator of reference 1 which showed greater low-frequency power and a drop to 1/100 of that power by about 80 hertz. However, dynamic distortion (6 rms) levels measured to 200 hertz and expressed as a percentage of the local steady-state pressure were about equal to those obtained in the present study.

The spectra of figure 9 exhibit some peaks which could be interpreted as either periodic or narrow-band random response. However, the amplitude probability density plots of figure 8 show no evidence of periodic content; therefore, the peaks in the spectra must be narrow-band random response. Reference 4 reports the one-dimensional-wave dynamic characteristics of this inlet. It was observed in that study that shock-position resonance occurs with internal bypass disturbances at frequencies of 85 and 180 hertz.

Some of the spectra of figure 9 show peaks at these frequencies; possibly the one-dimensional dynamics of the inlet was amplifying the random pressure fluctuations in a narrow band centered at the above frequencies. However, figure 9 also shows that these peaks were not highly prominent nor were they consistent for the various sensor locations or operating conditions. Therefore, there does not appear to be any significant relation between the distortion dynamics and the one-dimensional-wave dynamics of the inlet.

The peak-to-peak dynamic pressure levels obtained at each sensor location at the conditions shown in figures 8 and 9 were ratioed to the steady-state pressure levels at the compressor face station and are presented in figure 10 as a function of inlet pressure recovery. The peak-to-peak values were obtained as six times the rms values by assuming (as shown in fig. 8) that the data were random with a Gaussian amplitude probability density. Each rms value was obtained as the square root of the area under the appropriate power spectral density curve. As expected, figure 10 shows that the dynamic activity increased as the inlet operation became increasingly supercritical. This increased amplitude is particularly obvious for sensor b, which increased from about 9 percent at critical operation to about 18 percent at 13 percent supercritical operation. For an identical change in operation, the other sensors recorded somewhat lower values which increased from about 6 percent to about 13 percent. The corresponding steady-state distortions (fig. 6) were 18.6 and 32.7 percent, respectively. Therefore, the peak-to-peak pressure fluctuation amplitude (6 rms) at any one sensor was from 30 to 60 percent of the maximum steady-state spatial pressure variation.

SUMMARY OF RESULTS

Dynamic total-pressure measurements were obtained at several positions at the exit of a Mach 3 mixed-compression inlet. The inlet was operated at critical and various supercritical shock positions while at 0° angle of attack in the 10- by 10-foot supersonic wind tunnel. The cowl lip diameter was 45.98 centimeters. With sensors providing flat response to a maximum frequency of 200 hertz, the following preliminary results were obtained:

1. The amplitude probability densities of the pressure fluctuations were approximately Gaussian at all operating conditions and, therefore, the 6 rms value could be used as the peak-to-peak value.

2. Power spectral densities of the measured fluctuations decreased as frequency increased to 100 hertz and were fairly constant at higher frequencies. The initial drop in power density from 0 to 100 hertz averaged about 50 percent.

3. No resonant peaks were observed in the power spectral densities of the pressure fluctuations.

4. The peak-to-peak amplitudes (6 rms) of the pressure fluctuations were about 6 to 9 percent of the steady-state pressure during critical operation and increased to about 13 to 18 percent with the inlet operating 13 percent supercritically. These peak-to-peak amplitudes were from 30 to 60 percent of the maximum steady-state spatial pressure variations.

Lewis Research Center,
National Aeronautics and Space Administration,
Cleveland, Ohio, September 6, 1968,
126-15-02-11-22.

REFERENCES

1. Kimzey, W. F.: An Investigation of the Effects of Shock-Induced Turbulent Inflow on a YJ93-GE-3 Turbojet Engine. ARO, Inc. (AEDC-TR-66-198, DDC No. AD-377312L), Nov. 1966.

2. Stitt, Leonard E.; and Salmi, Reino J.: Performance of a Mach 3.0 External-Internal-Compression Axisymmetric Inlet at Mach Numbers From 2.0 to 3.5. NASA TM X-145, 1960.

3. Mitchell, Glenn A.; and Davis, Ronald W.: Performance of Centerbody Vortex Generators in an Axisymmetric Mixed-Compression Inlet at Mach Numbers From 2.0 to 3.0. NASA TN D-4675, 1968.

4. Wasserbauer, Joseph F.; and Whipple, Daniel L.: Experimental Investigation of the Dynamic Response of a Supersonic Inlet to External and Internal Disturbances. NASA TM X-1648, 1968.

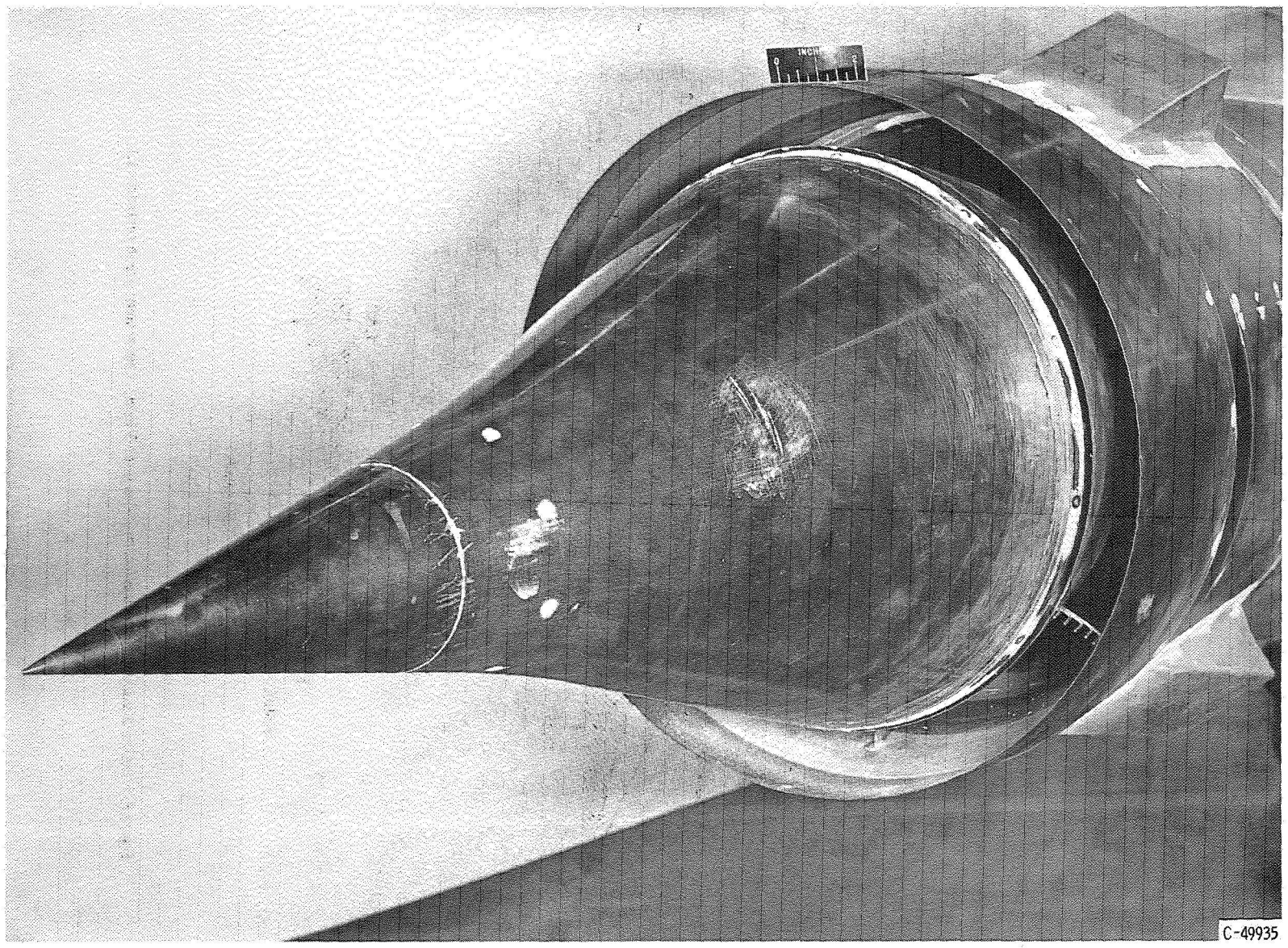

Figure 1. - Mach 3 mixed-compression inlet.

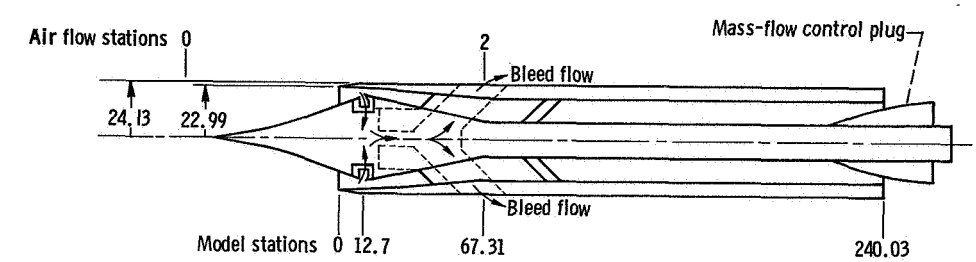

Model details

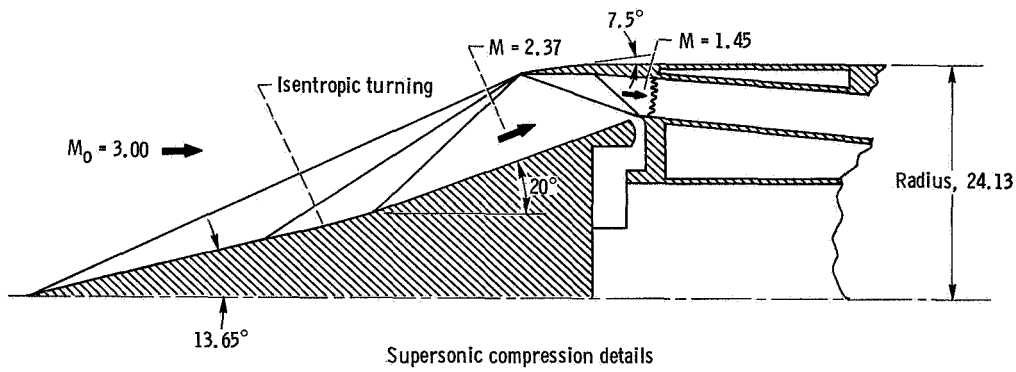

Supersonic compression details

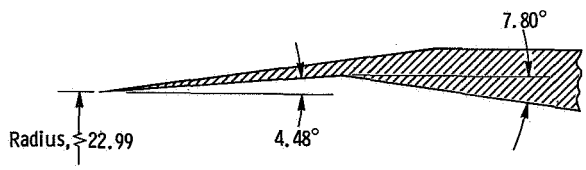

Cowl details

Figure 2. - Design of axisymmetric mixed-compression Mach 3 inlet. (Dimensions are in centimeters.)

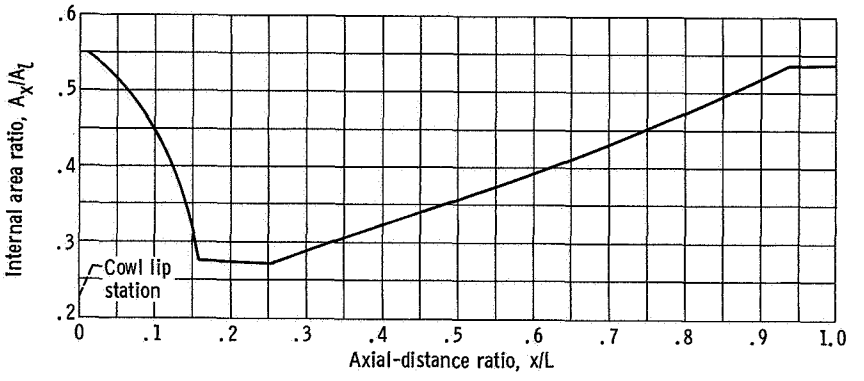

Figure 3. - Variation of diffuser internal area ratio at design conditions. Subsonic diffuser length, L, 73.8 centimeters.

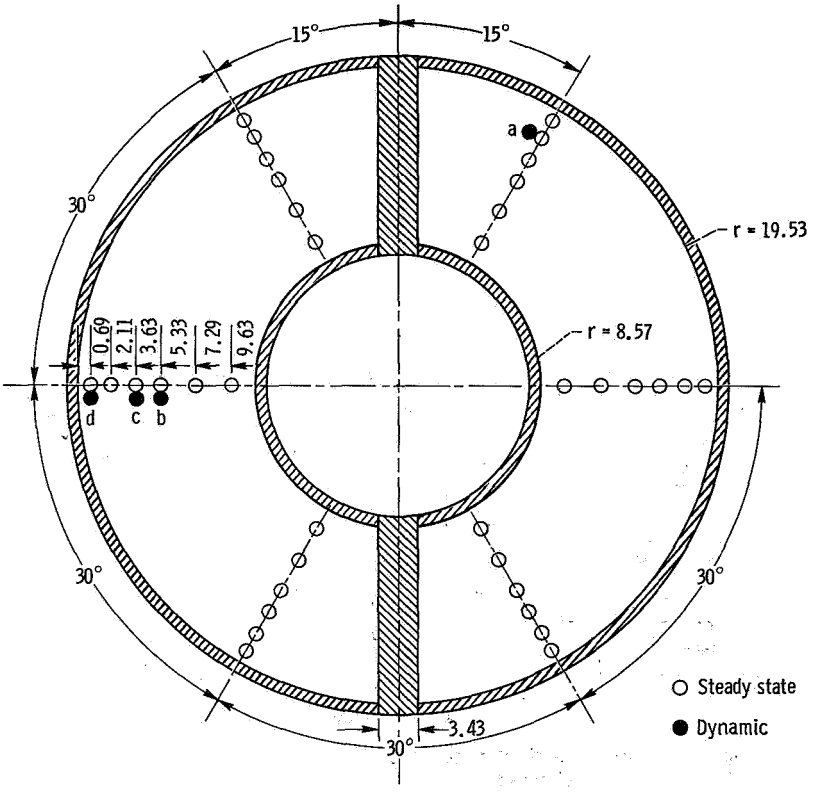

(a) Location of pressure sensors, looking downstream.

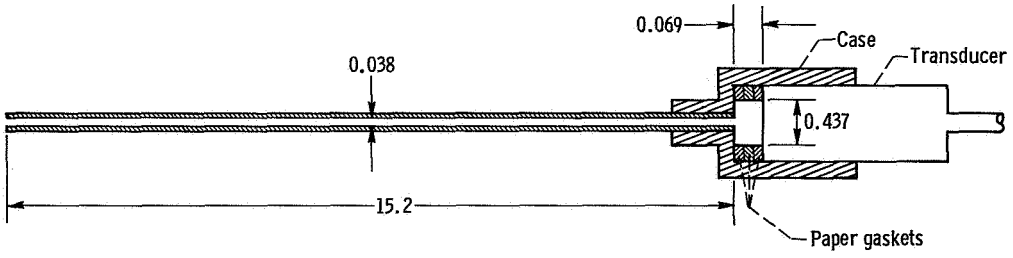

(b) Dynamic pressure-sensing system.

Figure 4. - Engine face instrumentation. (Dimensions are in centimeters.)

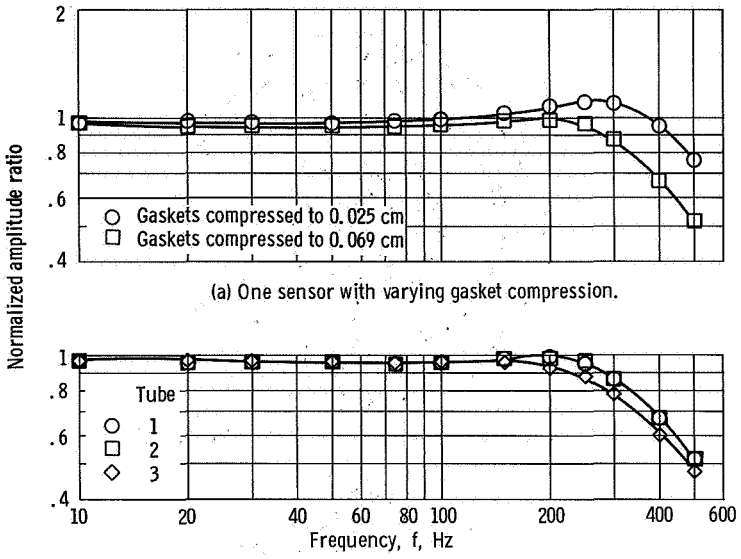

(a) One sensor with varying gasket compression.

(b) Three sensors with gaskets compressed to 0.069 centimeter.

Figure 5. - Frequency response of dynamic pressure-sensing system.

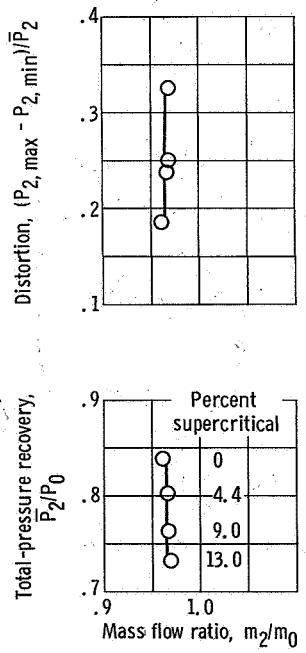

Figure 6. - Inlet performance at Mach 3.

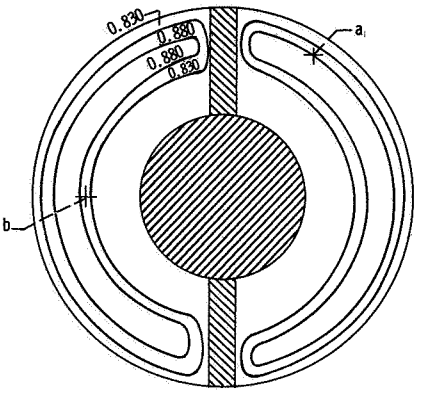

(a) Critical. Total-pressure recovery, 0.839; distortion 0.186.

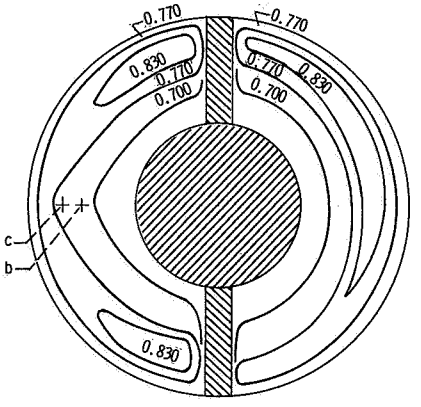

(b) Supercritical, 9 percent. Total-pressure recovery, 0.764; distortion, 0.250.

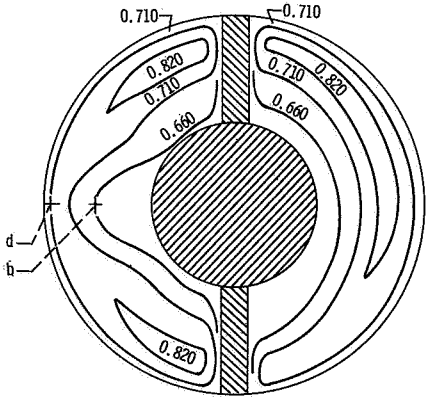

(c) Supercritical, 13 percent. Total-pressure recovery, 0.733; distortion, 0.327.

Figure 7. - Compressor face total-pressure contours.

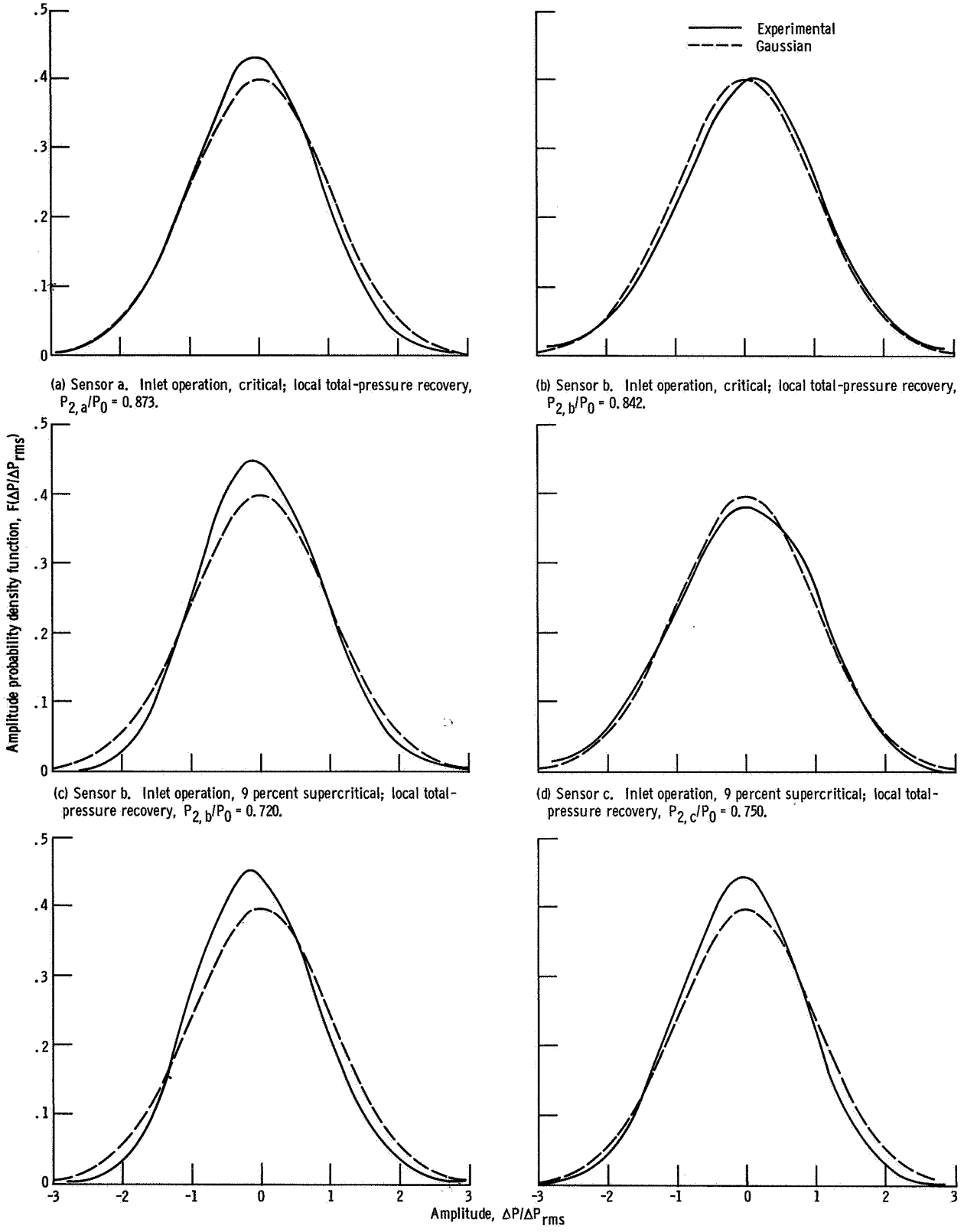

(a) Sensor a. Inlet operation, critical; local total-pressure recovery, $P_{2,a}/P_0 = 0.873$.

(b) Sensor b. Inlet operation, critical; local total-pressure recovery, $P_{2,b}/P_0 = 0.842$.

(c) Sensor b. Inlet operation, 9 percent supercritical; local total-pressure recovery, $P_{2,b}/P_0 = 0.720$.

(d) Sensor c. Inlet operation, 9 percent supercritical; local total-pressure recovery, $P_{2,c}/P_0 = 0.750$.

(e) Sensor b. Inlet operation, 13 percent supercritical; local total-pressure recovery, $P_{2,b}/P_0 = 0.654$.

(f) Sensor d. Inlet operation, 13 percent supercritical; local total-pressure recovery, $P_{2,d}/P_0 = 0.710$.

Figure 8. - Amplitude probability density of compressor face total pressure.

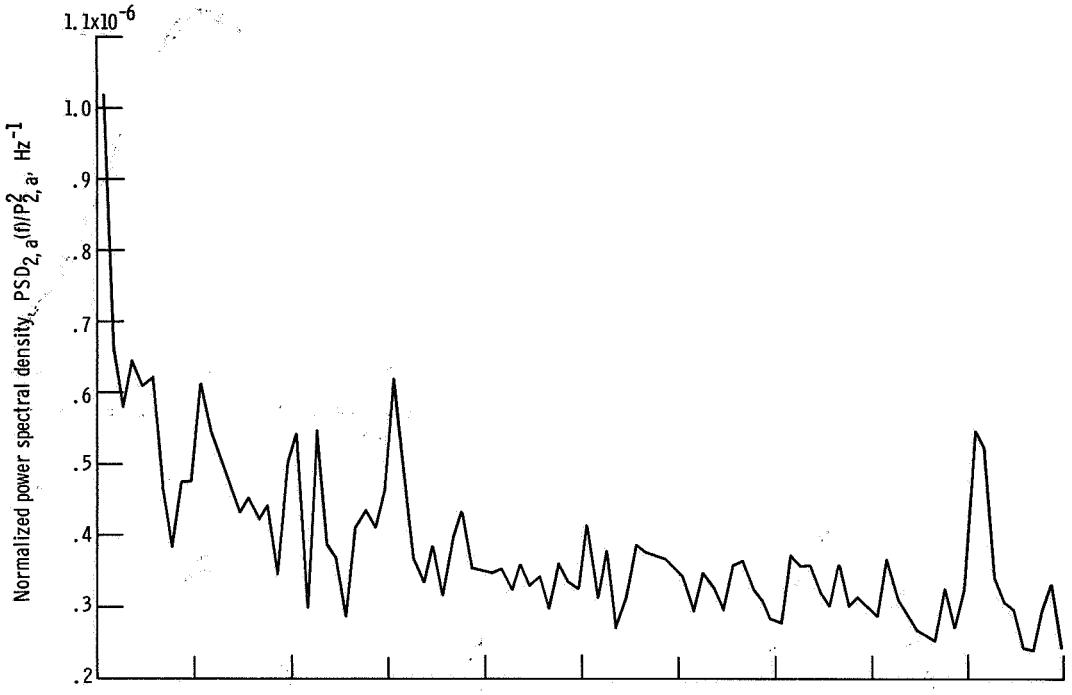

(a) Senosr a. Inlet operation, critical; local total-pressure recovery, $P_{2,a}/P_0 = 0.873$.

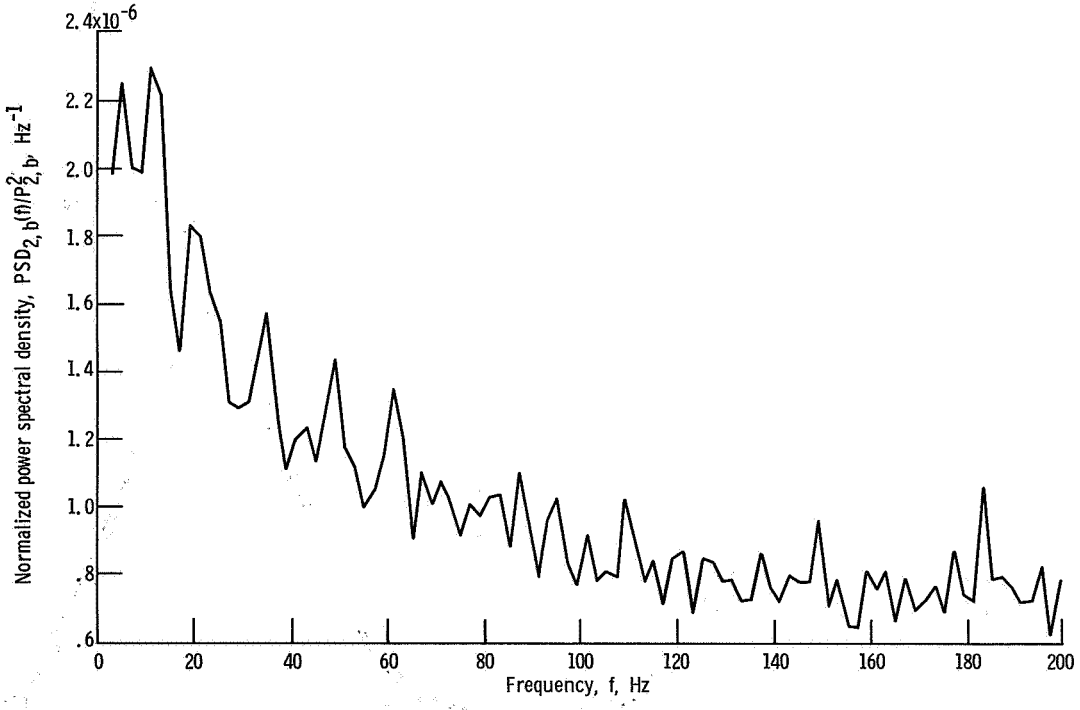

(b) Sensor b. Inlet operation, critical; local total-pressure recovery, $P_{2,b}/P_0 = 0.842$.

Figure 9. - Power spectral density of total pressure at simulated compressor face station.

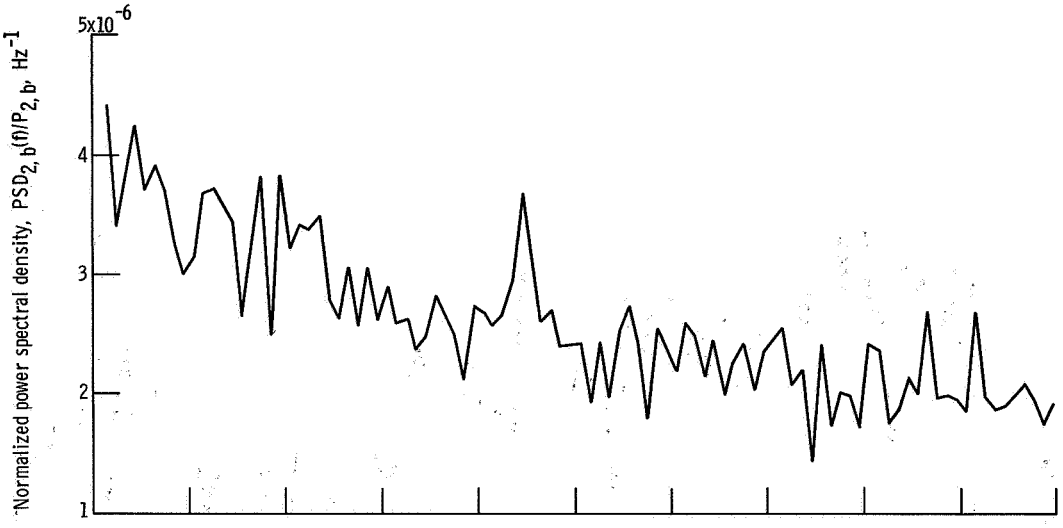

(c) Sensor b. Inlet operation, 9 percent supercritical; local total-pressure recovery, $P_{2,b}/P_0 = 0.720$.

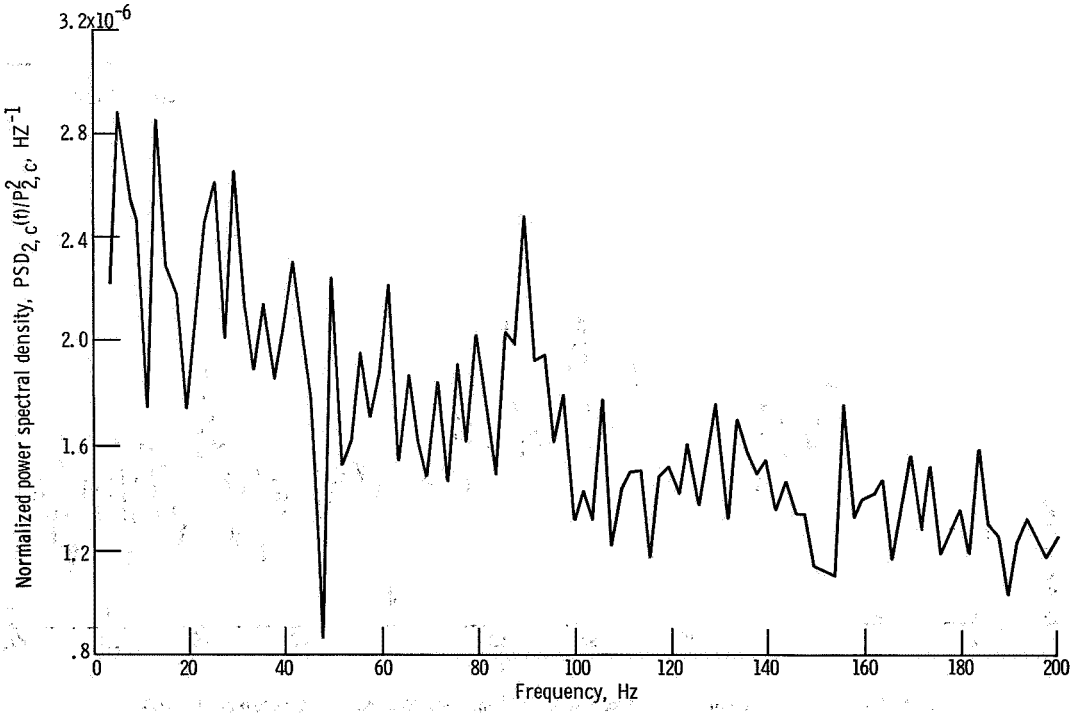

(d) Sensor c. Inlet operation, 9 percent supercritical; local total-pressure recovery, $P_{2,c}/P_0 = 0.750$.

Figure 9. - Continued.

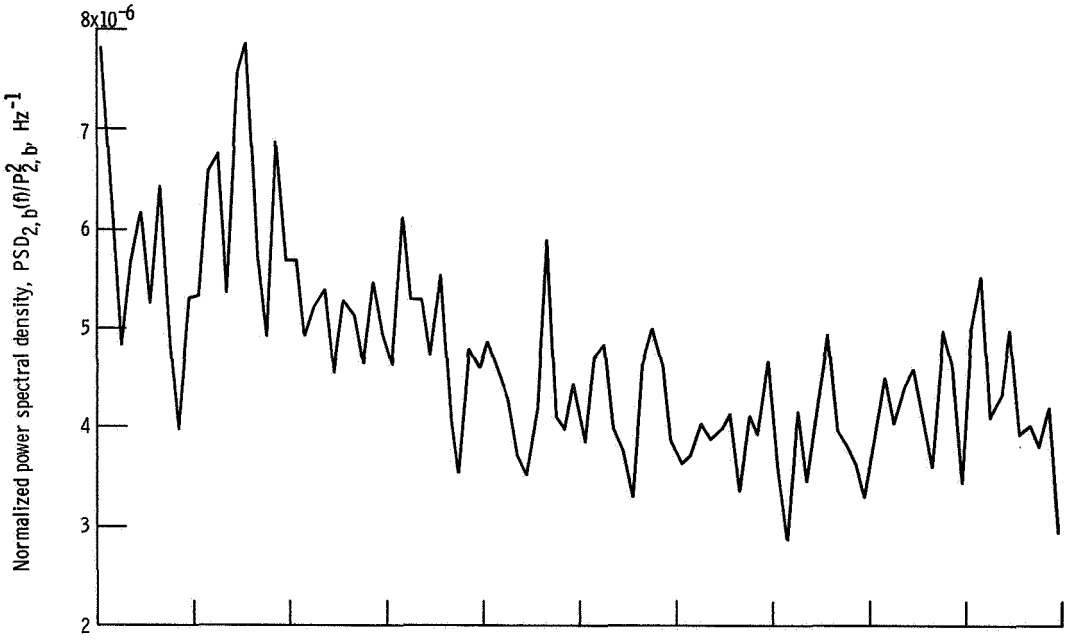

(e) Sensor b. Inlet operation, 13 percent supercritical; local total-pressure recovery, $P_{2,b}/P_0 = 0.654$.

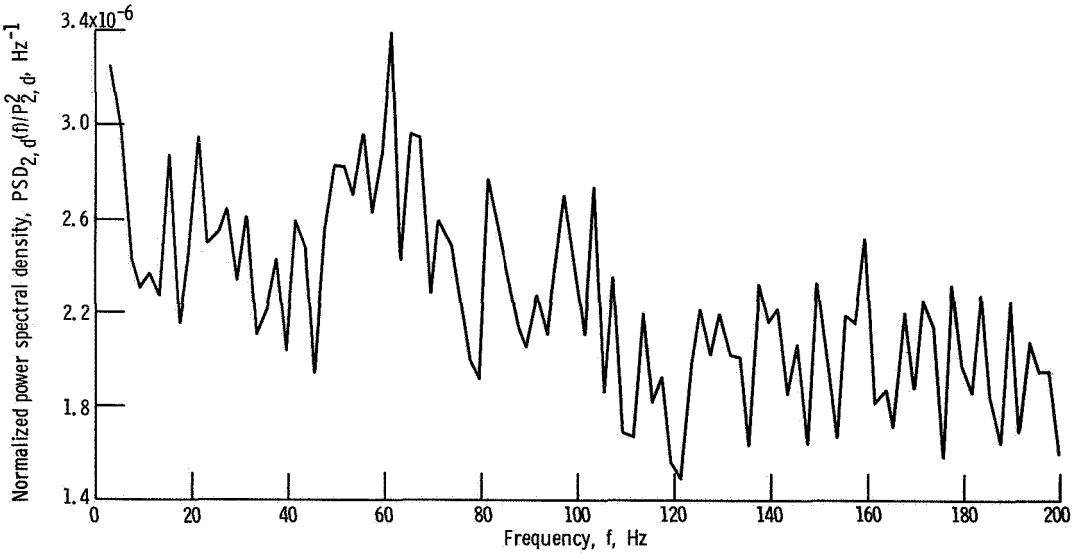

(f) Sensor d. Inlet operation, 13 percent supercritical; local total-pressure recovery, $P_{2,d}/P_0 = 0.710$.

Figure 9. - Concluded.

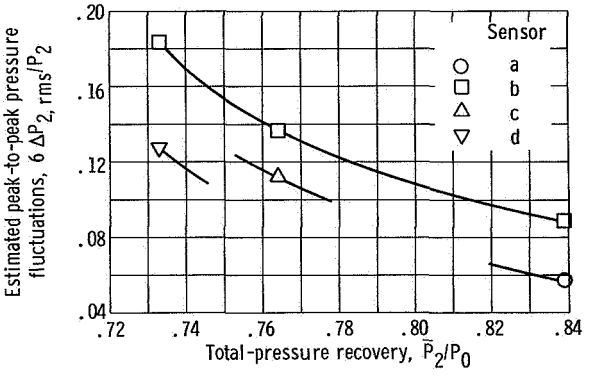

Figure 10. - Variation of estimated peak-to-peak pressure fluctuations with total-pressure recovery.

"The aeronautical and space activities of the United States shall be conducted so as to contribute . . . to the expansion of human knowledge of phenomena in the atmosphere and space. The Administration shall provide for the widest practicable and appropriate dissemination of information concerning its activities and the results thereof."

—NATIONAL AERONAUTICS AND SPACE ACT OF 1958

NASA SCIENTIFIC AND TECHNICAL PUBLICATIONS

TECHNICAL REPORTS: Scientific and technical information considered important, complete, and a lasting contribution to existing knowledge.

TECHNICAL NOTES: Information less broad in scope but nevertheless of importance as a contribution to existing knowledge.

TECHNICAL MEMORANDUMS: Information receiving limited distribution because of preliminary data, security classification, or other reasons.

CONTRACTOR REPORTS: Scientific and technical information generated under a NASA contract or grant and considered an important contribution to existing knowledge.

TECHNICAL TRANSLATIONS: Information published in a foreign language considered to merit NASA distribution in English.

SPECIAL PUBLICATIONS: Information derived from or of value to NASA activities. Publications include conference proceedings, monographs, data compilations, handbooks, sourcebooks, and special bibliographies.

TECHNOLOGY UTILIZATION PUBLICATIONS: Information on technology used by NASA that may be of particular interest in commercial and other non-aerospace applications. Publications include Tech Briefs, Technology Utilization Reports and Notes, and Technology Surveys.

Details on the availability of these publications may be obtained from:

SCIENTIFIC AND TECHNICAL INFORMATION DIVISION

NATIONAL AERONAUTICS AND SPACE ADMINISTRATION

Washington, D.C. 20546